

Immunization of Mice with AAV-mPTH or AAV-mPTH-GPI-Vector Vaccines Against A Parathyroid Hormone Induced Different T-Cell Proliferation Kinetics of Splenocytes



Anna Goncharenko¹, Ksenia Trutneva¹, Andrei Deviatkin², Aliko Yakovleva¹, Egor Ivlev¹, Pavel Belousov¹, Maria Vorontsova¹, Pavel Volchkov³, Galina Melnichenko¹, Natalia Mokrysheva¹ and Marina Loguinova^{1*}

¹Endocrinology Research Centre, Moscow, Russia

²Federal Research Centre for Innovator and Emerging Biomedical and Pharmaceutical Technologies, Moscow, Russia

³Life Sciences Research Center, Moscow Institute of Physics and Technology, National Research University, Dolgoprudny, Russia

Submission: June 24, 2024; Published: July 01, 2024

*Corresponding author: Marina Loguinova, Endocrinology Research Centre, Moscow, Russia.

Abstract

Parathyroid carcinoma (PC) is a rare neuroendocrine neoplasm characterized by excessive production of parathyroid hormone (PTH). Several reports demonstrated only a partial capability of PTH-targeted vaccination to control tumor progression in PC patients actualizing development of new strategies in PC treatment. The goal of this study was to develop adeno-associated viral (AAV) vector vaccines encoding mouse PTH (mPTH) in the native secreted form (AAV-mPTH) or in a glycosylphosphatidylinositol (GPI) anchored form (AAV-mPTH-GPI), and to investigate the immunogenic potential of both vaccines in laboratory mice. 7 weeks after two-stage intramuscular immunization of C57BL/6 mice at dose of 1×10^{11} viral genomes per mouse we studied mice splenocytes. ELISpot assay showed that stimulation of splenocytes with synthetic mPTH peptides binding ability of which with MHC molecules was calculated *in silico* did not induce mPTH-specific T-cell response. Polyclonal stimulation of splenocytes with anti-CD3/CD28 beads resulted in extensive expansion of T-cells among both vaccinated and control groups, while AAV-mPTH-GPI group demonstrated delayed T-cell proliferation kinetics as assessed via flow cytometry. We suppose that persistent presence of mPTH on cell surface can lead to tonic PTH-specific T-cell activation via cross presentation by dendritic cells, change activation threshold and ratio of T-cell subpopulations resulting in subsequent tolerance.

Keywords: AAV vector; AAV-mPTH; AAV-mPTH-GPI; Parathyroid carcinoma; Parathyroid hormone; Cancer vaccine; Immunogenicity; Immune tolerance; Delayed T-cell proliferation kinetics

Abbreviations: AAV: Adeno-Associated Virus; APC: Antigen-Presenting Cell; DC: Dendritic Cell; GPI: Glycosylphosphatidylinositol; PC: Parathyroid Carcinoma; PRR: Pattern Recognition Receptor; PTG: Parathyroid Gland; PTH: Parathyroid Hormone;

Introduction

Adeno-associated viral vectors (AAV vectors) encoding for a therapeutic transgene are one of the relevant technological platforms utilized for gene therapy of monogenic diseases [1-3]. AAVs are small, non-enveloped DNA viruses from the Parvoviridae family. Currently, AAVs are successfully used in gene therapy as a vehicle to deliver genetic material thanks to a number of their properties, such as their low immunogenicity, highly efficient transduction of cells and long-term expression in a safe episomal form without a high risk of inserting into the cell genome [4]. However, their usage in cancer immunotherapy

and the development of antitumor vaccines based on AAV vectors are limited due to the low immunogenicity of tumor-associated antigens as well as poor capability of AAVs to transduce antigen-presenting cells [5,6]. Depending on the goal of gene therapy, induction of T-cell response to the therapy transgene can either prevent reaching the therapy goal or favor it. AAV-based therapy of the congenital diseases with defective genes like hemophilia B requires a longstanding expression of the therapy gene, and the induction of T-cell response against either AAV capsid proteins or transgene is rather adverse as it may lead to the elimination of cells

expressing the transgene introduced with the AAV-vector [7,8]. T-cell response to the transgene would be extremely desirable if not a durational expression of the transgene is the issue but rather a prolonged T-cell response induced to it, specifically aimed, for example, at eliminating tumor cells generating the tumor-associated protein, an analogue of the transgene [9].

There are many factors that may impact the immunogenicity of a transgene delivered by AAV vectors. The magnitude of the immune response depends critically on the protocol. The method of the vector introduction [9,10], promoter type, the doses of vector; AAV serotype, the transgene itself and its epitopes, the target tissue and the structure of the vector genome are all of significant importance [11]. AAV vectors are characterized by efficient transduction of muscle fibers, but not antigen-presenting cells (APCs), including dendritic cells [6,12]. The advances of modern genetic engineering open the way of manipulating the immunogenicity to the transgenes delivered with AAV-vectors - either reducing it in the case of gene therapy of congenital hereditary pathologies, or on the contrary, increasing it in developing antitumor vaccines. Thus, AAV vectors are recognized as a potential platform for the development of antitumor vaccines, and particularly for parathyroid carcinoma (PC).

PC is a rare neuroendocrine neoplasm characterized by a malignant transformation of one or more parathyroid glands (PTG) [13,14]. Patients with PTG tumors characteristically exhibit an excessive production of parathyroid hormone (PTH) that leads to the development of high-level hypercalcemia and multiple complications - osteoporosis, pathological fractures, fibrocystic osteitis, urolithiasis [15]. PC demonstrates aggressive behavior with high potential for metastasis. To date, the only effective PC therapy is the surgical removal of the transformed glands and tissues, but in the case of surgery at the late stage accompanied by metastases, the effectiveness of the operation is reduced [16]. The prognosis for the successful treatment for PC depends on the completeness of removal of the malignant area. Unfortunately, despite careful surgery and complete resection of tumor, relapses occur in more than 50% of cases [17]. There is still no specific therapy that can be used to treat patients with metastatic relapses. These patients are at risk of an unfavorable prognosis due to the uncontrolled, severe, and drug-resistant hypercalcemia caused by the elevated level of PTH produced by metastatic tumor cells. Patients often die not from tumor invasion, but from the excessive production of PTH and its metabolic consequences.

Since PC is resistant to radiotherapy and chemotherapy, new approaches of gene and immunotherapy are of great interest. But research and clinical data regarding PC immunotherapy is scarce. One approach in PC immunotherapy aimed at reducing the pathologically high metabolic activity of PTH might be the immunization with synthetic human PTH peptides able to induce the formation of neutralizing autoantibodies to PTH, thus alleviating its pathological manifestations. The literature describes

several clinical cases of peptide immunization against PTH with varying degrees of success [18-20]. B-cell tolerance to human PTH was overcome by multiple immunizations with human intact PTH mixed with synthesized modified human PTH peptides (with a random substitution of one amino acid), foreign antigens (bovine PTH peptides), and reconstituted in Freund's complete adjuvant. An interesting case is known regarding a 24-year-old patient who had a long-term 12-year remission of the disseminated lesion after the combined therapy via immunization and subsequent surgical treatment [21]. However, the mechanism of remission and molecular factors that could regulate the effectiveness of PC immunotherapy have still remained unclear. It should be noted that peptide immunization could cause not only a humoral response, but also a T-cell response. Moreover, depending on the dose, mode and the route of peptide administration, the opposite T-cell response can be observed - from priming to tolerance induction [22].

Another immunotherapeutic approach also employed in PC therapy was based on the using of dendritic cells (DCs) of the patient, isolated from his mononuclear cells. After DC and PTH interaction *in vitro*, DCs present on their surface PTH peptides in complex with MHC (major histocompatibility complex) class 1, and become able to stimulate tumor-specific CD8 T cells. The 50-year-old patient was treated with multiple courses of immunizations with DCs loaded with PTH peptides - 4 injections once a week and 10 injections on a monthly basis [23]. After vaccination, she had a PTH-specific immune response *in vitro* and *in vivo* (delayed hypersensitivity reaction) along with decreased serum PTH levels. But during the therapy, there was no reduction of the tumor mass.

Therefore, at present, there is still a limited number of attempts of successful PC immunotherapy, which makes the issue of developing a gene therapeutic vaccine still a concern. AAV vector vaccine encoding for PTH typically produced by PTG cells and abnormally elevated in PC, could lead to PTH-specific T-cell response, which in turn could induce the elimination of malignant PC cells thus reducing PTH levels. It is interesting that in 2022 Burr et al first obtained AAV vectors encoding for the full-genome version of the human PTH gene (1-84), though with the aim of their potential use in the hypoparathyroidism treatment [24]. There exist few other gene therapy models for hypoparathyroidism that utilize PTH delivery systems other than AAV [25,26].

In this study we developed 2 different AAV-vectors encoding for mouse PTH (mPTH). One variant of the AAV-vector encoded for mouse PTH (mPTH) in the native secreted form (AAV-mPTH), and the other variant was a modified mPTH version able to bind to a glycosylphosphatidylinositol (GPI) anchor (AAV-mPTH-GPI) during the posttranslational modification, which leads to mPTH attachment to the membrane of the transduced cells. The transgene plasmids and AAV-vectors were constructed using standard techniques of genetic engineering. The mPTH

expression in vectors was verified in transduced HEK293T cells using fluorescence microscopy and qPCR. C57BL/6 mice were immunized intramuscularly either with AAV-mPTH-vector or AAV-mPTH-GPI-vector, twice within a 2-week interval; first with AAV2 serotype and then with AAV9 serotype. 7 weeks after the boost, the animals were euthanized. T-cell response to the immunization was evaluated by changes in the relative numbers of lymphocyte subpopulations among splenocytes by flow cytometry using BD FACS Aria III. ELISpot assay was used to estimate PTH-specific T-cell response after stimulating splenocytes with a mixture of synthetic mPTH peptides. The library of mPTH peptides with high affinity binding to MHC molecules of C57BL/6 mice was built *in silico* using the NetMHCIIpan-4.0 software module. The proliferative potential of CFSE-labeled splenocytes stimulated either specifically with a pool of peptides to mPTH or nonspecifically with anti-CD3/CD28 particles was assessed by flow cytometry.

Our study showed that 7 weeks after two-stage intramuscular immunization of C57BL/6 mice at a dose of 1×10^{11} viral genomes per mouse, the group vaccinated with AAV-mPTH-GPI significantly differed from the other groups. The relative number of CD4+ T-cells decreased significantly while the relative number of activated CD4+CD25+ T-cells increased in the spleens of AAV-mPTH-GPI-vaccinated mice compared to the control and AAV-mPTH vaccinated groups. The number of regulatory T-cells expressing CD25+FoxP3+ and CD25+CD127 low did not differ significantly through the groups. The stimulation of splenocytes from the vaccinated mice with the synthetic murine PTH peptides did not induce T-cells to secrete IFN γ or promote the proliferation of specific clones. Polyclonal stimulation of splenocytes with anti-CD3/CD28 beads resulted in an extensive expansion of T-cells among both vaccinated and control groups, but in the AAV-mPTH-GPI vaccinated group T-cell proliferated more slowly. Only 43% of the cells have divided by the third day of the analysis in the AAV-mPTH-GPI-vector vaccinated group, while the control group of mice demonstrated 79.4% of the proliferating cells, and 77.6% were in the group of the splenocytes from the mice vaccinated with the AAV-mPTH-vector. The differences in the cell frequencies between the control and mPTH-GPI groups were statistically significant ($p = 0.0022$). There were no significant differences between the mPTH and control group ($p = 0.697$) and between the mPTH-GPI and mPTH groups ($p = 0.1255$).

Therefore, in our work we took the first step in developing an AAV-based gene therapy vaccine aimed at initiating PTH-specific T-cell immune response able in a model of PC to eradicate PTH-producing tumor cells. We used AAV vectors in 2 modifications and estimated their immunogenicity in response to synthetic PTH peptides whose binding ability with MHC molecules was calculated *in silico*. We discovered that both variants of AAV-vectors were non-immunogenic, and moreover, AAV-mPTH-GPI variant led to rather polyclonal tolerance of T cells. Many studies demonstrate the induction of tolerance to the transgene in response to AAV-

vector immunization [27-31]. We suppose that the persistent presence of PTH on the cell surface, mostly on myocytes due to their prevalence in the muscle tissue, can lead to weak and tonic PTH-specific T-lymphocytes activation via cross-presentation by dendritic cells and development of subsequent tolerance.

Materials and Methods

Reagents

Dulbecco's Phosphate-buffered Saline without Ca&Mg, without phenol red (DPBS 1x, Capricorn, Germany), RPMI 1640 Medium with L-Glutamine (Capricorn Scientific, Germany), Dulbecco's Modified Eagle Medium High Glucose (4.5 g/L) (DMEM, Capricorn Scientific, Germany), Fetal Bovine Serum (FBS, Gibco/ThermoFisher Scientific, USA), GlutaMax (Gibco/ThermoFisher Scientific, USA), Penicillin/Streptomycin (10000 Units/mL Penicillin, 10000 μ g/mL Streptomycin, Gibco/ThermoFisher Scientific, USA), Interleukin 2 IL-2 (R&D Systems, USA), Trypan blue (BioRad, USA), 2-mercaptoethanol (2-ME, Helicon, Russia), ammonium chloride (NH $_4$ Cl, Helicon, Russia), HEPES (Paneco, Russia), gentamicin (Paneco, Russia), sodium pyruvate (Paneco, Russia), Dimethyl sulfoxide (DMSO, Serva, USA), sodium bicarbonate (NaHCO $_3$, Sigma-Aldrich, USA) and EDTA (Panreac AppliChem ITW Reagents BioChemica, Spain).

The construction of a plasmid encoding murine PTH

In order to construct the gene encoding mouse parathyroid hormone (mPTH, *Mus musculus*, NCBI Reference Sequence: NM_020623.2) and consisting of two exons, two fragments of 96 and 262 bp were obtained and fused using overlap extension PCR to produce the final fragment of the complete gene of 366 bp. Genomic DNA isolated from the pluripotent cells of C57BL/6 mice with the ExtractDNA Blood & Cells kit (Evrogen, Russia) was used as a template. The shorter fragment of 96 bp was obtained through annealing of oligomers of the following sequence:

mPTH_olig_F (73-mer):

ctcacgggtttcccatcctgttggttaagaagacagactgccagcatgatgatcatcatcttagccacgggtg

mPTH_olig_R (73-mer):

tttctcttttagtaaatgatgtctgcaaacaccgtgctaaagtgatgatcatcatgctggcagctctgtc

The longer fragment of 262 bp was obtained via PCR with the following primers:

mPTH_s1_F: ttactgagattttgatttaactaatacatccacatcagc

mPTH_s1_R: gaagagagctgtcagtgaaatacagcttatgca

Then overlap extension PCR was used to fuse both fragments and to add restriction sites for Age2 and Ecor1 restriction endonucleases using the following primers:

mPTH_s2_plus_Ecor_F: atcttttattgaattcttactgagatgttgatttaactaatatccacatcagc

ovlp_mPTH_s1_s2_F: cagctctctctccacgggttcccatcgc

ovlp_mPTH_s1_s2_R: gaaaccctgaggaagagagctgctcagtgaaatac

mPTH_s2_R_plus_Age_R: tacaccggcgccacttctctttagtaagatgatgctgcaaacacc

Upon construction of a complete fragment of the gene expressing murine PTH (mPTH), it was inserted into a plasmid for the assembly of adeno-associated viruses (AAV2/2). The packaging plasmid for the AAV assembly was ordered from Addgene. The final plasmid is shown in Figure S1A.

The second plasmid had the mPTH fragment identical to the previous one, but with a 91 bp extension that encodes glycosylphosphatidylinositol (GPI) anchor signaling sequence directing the mPTH into the endoplasmic reticulum. The C-terminal signaling sequence is cleaved off and replaced by the GPI-anchor during the process of the post-translational modification, thereby converting the secretory form of mPTH into a GPI-anchored form that remains attached to the cell membrane [32] GPI-anchor was produced via annealing oligonucleotides of the following sequence:

GPI_olig_F: Cttgaaaatggtgggacatcctatcagagaaaacagttctctgctggtgactccattctggcagcagcctg

GPI_olig_EcoR_R: Gaattctccttaggatgaaggctccagctgctccagaaatggagtcaccagcagaagaactggtt

The final packaging plasmid producing mPTH so that it stays attached via GPI-anchor to the membrane of transduced cells is shown in Figure S1B.

Plasmids were produced in the E. coli culture (XL10-Gold Ultracompetent Cells). Plasmid DNA was isolated with the Plasmid Midiprep 2.0 kit (Evrogen, Russia) as per the manufacturer's protocol. The concentration of plasmids was measured after two cycles of DNA precipitation in an alcohol. The final plasmids had mPTH transgene with or without GPI-anchor sequence, a strong core EF-1 α promoter, flanked at both ends by ITR sequences of the AAV2 serotype.

AAV-vector assembly

AAV-vectors were produced in a standard way [33] with modifications. They were assembled in Human embryonic kidney cells (HEK)293T cells by co-transfection of the transgene plasmid, helper pAdDeltaF6, and RepCap plasmid of AAV. 10x10⁶ HEK293T cells were seeded on Petri dish (150x20 mm) and left to adhere within 24 hrs before cotransfection in DMEM culture medium containing 4.5 g/L glucose, 10% FBS, 1% GlutaMax, and 1% gentamicin. The mixture of triple plasmids used at a weight of 38 μ g each at a molar ratio of 1:1:1 per a Petri dish contained the transgene plasmid, helper pAdDeltaF6, and RepCap plasmid of AAV. Plasmids were incubated with a final concentration of 0.075 mg/ml in acidified l-PEI (linear polyethylenimine, 25000 MW, 5 mg/mL) in lactate buffer (20 mM sodium lactate, 150 mM sodium chloride) at a ratio 1:1 (vol:vol) within 20 min at RT and then added to the growth medium supplemented with 2% FBS at a ratio 1:12.5 (vol:vol). HEK293T growth medium was replaced with the

new transfection medium that contained triple plasmids. After 72-hour transfection, AAV-vectors were isolated from HEK293T cells by lysis (150 mM NaCl, 50 mM Tris-HCl, 1 mM MgCl₂, pH 8.5, 0.5 Triton X-200, benzonase 50U/ml). Homogenates were purified by discontinuous iodixanal gradient ultracentrifugation, followed by ultrafiltration using Amicon Ultra-15 filters (Merck Millipore, USA). The titer of AAV-vectors was calculated using real-time PCR (qPCR) on a Multicolor Real-time PCR Detection system iQ5 amplifier (BioRAD, USA).

Total RNA was extracted with RNeasy Mini Kit (Qiagen, Germany). qPCR was performed to calculate virus titre using primers to GFP fused to mPTH: 5'-AGATCCGCCACAACATCGAG-3' and 5'-GGTAGTGGTTGTCGGGCAG-3', as well as primers directly to mPTH: 5'-GCACAACCTGGGCAAACACCTG-3' and 5'-TTGGTGGGCTTCTGGTGACTG-3' and probe 5'-AGGATGCAATGGCTGAGAAGGAAGCTGC-3'. The qPCR protocol for assessing the titer of viral particles included: 3 min of denaturation at +95°C, 39 cycles of 15 sec denaturation at +95°C, followed by annealing and elongation at +58°C for 20 sec.

Cell Lines. Cultivation and transduction *in vitro*

HEK293T were passaged and maintained in 6-well plates with 25% confluency in a standard DMEM-based growth medium with 10% FBS, 1% GlutaMax, 1% penicillin/Streptomycin solution. The next day upon cell attachment the medium was changed with a fresh one without antibiotics, and AAV-vectors were added in a range of 200 to 20000 vg (viral genomes) per cell. After 24-hour incubation, the medium was replaced with a fresh complete growth medium. On day 3 following transduction GFP-positive cells were inspected with EVOS M5000 Imaging System microscope (Thermo Fisher).

Mice

C57BL/6 mice were obtained from the Branch of the Institute of Bioorganic Chemistry, Russian Academy of Sciences (Pushchino, Moscow region, Russia). Male mice aged 2 months were used for all studies. The mice were held in an animal facility of Endocrinology Research Centre in IVC in a temperature- and humidity-controlled room (temperature 21 \pm 2°C and humidity 55 \pm 5%) with a 12 h light/dark cycle. Animal health and behavior were monitored daily by animal facility personnel.

The mice were split into 3 experimental groups, with 5 animals in each group. The control group was injected intramuscularly (m.quadriceps femoris) with 50 μ l of pure buffer. A single intramuscular injection of AAV-mPTH and AAV-mPTH-GPI vectors, the serotype AAV2, was given to mice with a dose of 1x10¹¹ viral genomes per a mouse in first and second groups. Two weeks later a boost vaccination with the serotype AAV9 of the same titer was administered intramuscularly to both experimental groups. The control group was again injected only with 50 μ l of pure buffer. 7 weeks later all mice were euthanized by cervical dislocation and removed from the experiment.

A single intramuscular injection, performed by an experienced and qualified personnel, was considered low severity procedure. AAV vectors have an excellent safety record in clinical trials and preclinical animal studies [34,35]. In this regard, the experimental design does not involve humane endpoints.

Isolation of Mice Splenocytes

Splenocytes were isolated according to the protocol by Michels et al [36], with some modifications. Cell suspensions from spleens were generated via delicate grinding by the flat side of a syringe plunger through a 70- μ m pore size strainer (Miltenyi Biotec, Germany) into a tube with cold DPBS, rinsing the strainers with DPBS several times. Upon centrifugation at 300 g, 4°C, for 10 minutes the pellets were resuspended in RPMI 1640 medium supplemented with 10% FBS, 0.05 mM 2-ME, 25 mM HEPES, 1 mM sodium pyruvate, 1% Glutamax, 1% 100 U/ml penicillin, 100 mg/ml streptomycin, and washed again. Then the cell pellets were treated with 3 ml Red Blood Cell (RBC) Lysis Buffer based on ammonium chloride. Lysis performed at +4°C for 3-5 minutes was terminated with 9 mL growth medium and two washes at 300g at 4°C for 10 minutes. The splenocyte sediment was resuspended in 1 ml of medium; the number of cells was determined using a TC-20 cell counter (Biorad, USA), with 0.4% trypan blue solution added to assess cell viability. Splenocytes resuspended in FBS with 10% DMSO at a final concentration of 10×10^6 cells/mL were placed in Corning CoolCell LX cell freezing containers and frozen at -80°C. 1-7 days later the cells were transferred into liquid nitrogen. The day before the experiment the cells were defrosted in a water bath at +37°C, transferred into the growth medium with 5 ng/ml IL-2, and kept overnight in a CO2 incubator (Binder, Germany).

Flow cytometry

Splenocytes were stained in a standard way with the following fluorescent-labeled antibodies: anti-CD3-PerCP-Cy5.5 (1:50 dilution, clone 17A2, BD Biosciences, USA), CD127-PE-CF594 (1:50 dilution, clone 3B/199, BD Biosciences, USA), CD4-VioBlue (1:50 dilution, clone REA604, Miltenyi, Germany), CD25-APC (1:50 dilution, clone REA568, Miltenyi, Germany), FoxP3-PE (dilution 1:50, clone REA788, Miltenyi, Germany). Briefly, a mixture of antibodies to surface antigens was added to 100 μ l of a cell suspension containing 1.5×10^6 cells in MACS buffer consisting of 1xDPBS, BSA 0.5%, EDTA 2 mM and incubated for 30 min at 4°C. Then, the cells washed with MACS buffer from the unbound antibodies were fixed and permeabilized with fixation and permeabilization buffers according to the manufacturer's protocol (Treg Analysis Kit, with FoxP3-PE, anti-mouse, REAfinity, cat 130-120-674, Miltenyi, Germany), and stained with intracellular FoxP3. Flow cytometric measurements were performed on a BD FACS Aria III cell sorter (BD Biosciences, USA), detecting at least 30000 events in the lymphocyte gate. Positive events and the boundaries of positive gates for CD127 and FoxP3 were set using FMO-control "fluorescence minus one". Dead cells were removed from the analysis using a signal from 7-AAD (Abcam, UK), along with removing highly granular and small events on the FSC/SSC

dot plot. Data analysis was carried out using FlowJo v10 software.

ELISpot assay

T-cell immune response was assessed by IFN γ production after stimulation using ELISPOT kit (Cellular Technology Limited (CTL), Shaker Heights, USA) in accordance with the manufacturer's protocol. In brief, 2×10^5 splenocytes from each animal, in 2 replicates, were added per well, earlier coated with anti-mouse IFN γ antibodies, in the CTL culture medium supplied with the ELISpot kit, and supplemented with 1% Penicillin-Streptomycin, 1% Glutamax and 0.05 mM 2-ME. The cells were stimulated with either peptide pool to mPTH at two concentrations, 10 μ g/ml and 100 μ g/ml, or 10mg/ml phytohemagglutinin (PHA-P) (Paneco, Russia) used as a positive control. Anti-mouse CD28, 1 μ g/ml per well (from the T Cell Activation/Expansion Kit, mouse Miltenyi Biotec, Germany) was added into some wells to provide additional co-stimulatory signal to TCR challenged with mPTH peptides. Cells without any stimulating agents served as negative control. Plates with cells were incubated for 18 hours at 37°C with 5% CO2. Then, the cell suspension was rinsed, and the membrane was washed twice with DPBS, and incubated with anti-mouse IFN γ -biotinylated antibody for 2 hours in the dark at RT. Next, the membranes were washed again to remove the unbound antibodies and incubated with the manufacturer's streptavidin solution for 30 minutes in the dark at RT. Finally, the membranes were washed and incubated with the Blue developer solution for 15 minutes in the dark at RT. Afterwards, the plates were rinsed with distilled water, with the back of the membrane washed as well, and left to dry overnight. IFN γ spots were detected and counted using a CTL Imager ImmunoSpot analyzer (Cellular Technology Limited, Shaker Heights, USA). The results are presented as a number of spots per well.

Proliferation assay

Splenocyte proliferation was analyzed by the fluorescent signal of Carboxyfluorescein Succinimidyl Ester (CFSE, BD Biosciences, USA) diluted proportionally to cell proliferation and detected with flow cytometry. CFSE labeling was performed according to the manufacturer's protocol with some modifications. In brief, the cells were transferred from the growth medium into warm DPBS (37°C) with 0.1% FBS (below referred to as DF) via two washes in DF at 300 g, 10 min, RT. Next, equal volumes of the cell suspension with 1×10^6 cells in DF and CFSE were mixed to 0.1 μ M CFSE as a final concentration and incubated in 5% CO2 for 5 minutes. The reaction was stopped with a 9-fold volume of the cold growth medium and 2 washes at 300g for 10 minutes at 4°C. CFSE-labeled cells were left in a growth medium with 1% FBS without IL-2 for 4 hours to synchronize the cell cycle phases and to stabilize CFSE staining intensity that is 1-log decreased due to natural efflux of CFSE-bound proteins from the cells or degradation of some short-lived proteins [37]. Synchronized cells washed with the growth medium were transferred into a 96-well U-shaped plate (Corning, USA), 5×10^4 cells per well in 100 μ l of medium. Additional 100 μ l of medium supplemented with 5 ng/ml IL-2 was added to

wells with the negative control (not stimulated cells). Stimulation agents (CD3/CD28 particles or a pool of mPTH peptides) mixed separately in the medium with 5 ng/ml IL-2 were added to the experimental wells with cells in a volume of 100 μ l. Non-specific stimulation of the T-cells was achieved with anti-CD3/CD28 particles (T-Cell Activation/Expansion Kit, mouse Miltenyi Biotec, Germany) in accordance with the manufacturer's protocol. First, a suspension of particles conjugated with CD3 ϵ -Biotin and CD28-Biotin antibodies was prepared to a final particle concentration of 1×10^5 particles/ μ l. Before stimulation of the cells the particles were transferred to the growth medium and added in a volume of 100 μ l to the wells with cells in a ratio of 0.5:1 (particles:cells). The cells were stimulated within 72 hours. CFSE fluorescence intensity was measured using a BD FACS Aria III cell sorter (BD Biosciences, USA). CFSE histograms were analyzed using FlowJo v10 software. Specific stimulation of the mPTH-specific TCRs was performed with the pool of mPTH peptides.

Peptides

The peptide library of 26 murine PTH peptides was built based on the analysis of the peptides binding to and their presentation by major histocompatibility complex (MHC) molecules of C57BL/6 mice. The peptides were generated using the Uniprot resource. NetMHCIIpan-4.0 and NetMHCpan-4. software modules were used to calculate the probability of the mPTH peptides binding (or affinity) to MHC molecules of C57BL/6 mice. The peptide library was composed of the overlapping peptides covering the entire mPTH sequence. There were 26 peptides in total, each of 15 amino acids (AA) by length, with the adjacent peptides overlapping by 11 AA - Table S1. The peptides numbered 1, 2, 3, 8, 9, 12, 13, 14, 16, 17, 23 and 24 showed binding ability to MHC class I as predicted by NetMHCpan - 4.1. Peptide 17 could also bind to MHC class II as predicted by NetMHCIIpan - 4.0. Peptides 15 and 17 had motifs overlapping with those of the predicted peptides with a high binding capacity to MHC molecules. The peptides in lyophilized form were provided by Verta, LLC (St. Petersburg, Russia).

Statistical Analysis

Statistical analysis was performed with GraphPad Prism software ver. 6.01 (GraphPad Inc, USA). Data in all histograms and tables are represented as median values with IQR (interquartile range). The Mann-Whitney U test was used to assess statistical significance of differences between two independent groups. Data were considered significantly different at p values <0.05. The significance level and p values are shown as * (p < 0.05) between control and mPTH-GPI; ** (p<0.05) between control and mPTH; *** (p<0.05) between mPTH and mPTH-GPI.

Results

Generation of AAV vectors containing murine mPTH gene, either in its secreted form (mPTH) or in its modified form (mPTH-GPI)

The methodology for the production and purification of

AAV vectors has been described elsewhere [33,38]. A complete fragment of the gene encoding murine PTH (mPTH) was inserted into a plasmid used as a therapeutic plasmid to assemble AAV vectors (Figure S1A). Another variant of a therapeutic plasmid had the identical mPTH gene, but it was fused to the signal sequence of 91 bp of a glycosylphosphatidylinositol (GPI) anchor (Figure S1B) that is usually replaced by GPI-anchor during post-translational modification rendering mPTH attached to the cell membrane and preventing it from the exit into the extracellular space [32]. The attachment of normally secreted proteins to the cell membranes is often used during the elaboration of cancer and other vaccines to manipulate the direction and magnitude of the immune response [39]. Thus, the trapping of cytokine and co-stimulatory molecules or growth factors on the membrane surface usually induces a stronger immune response to the vaccine's antigen [32,40] while the integration of proteins that don't typically regulate the immune response can affect immune reactions to this protein [41]. As the half-life of PTH in the blood is 3-4 minutes [42], and up to 2 hours for the recombinant human PTH [43], we proposed that modification with GPI anchor would provide more prolonged life of mPTH on the membranes of transduced cells.

The efficiency of cell transduction with the AAV vector contained AAV-mPTH was tested in HEK293T cells using AAV vectors with GFP; the results are shown in Figure S2. The expression of mPTH in AAV vectors was assessed in HEK293T cells by qPCR; doses of the vectors ranged from 500 to 20000 ng.

Laboratory Animal Immunization

The C57BL/6 mice were split into 3 groups, each of 5 mice. The initial vaccination was given with AAV2 serotype, while AAV9 serotype was used in a booster immunization, with a dose of 1×10^{11} viral particles per mouse in both vaccinations. The dose was determined based on the study by Burr et al. on the dose response of the transgene production in a mouse model, though the AAV vector was administered intravenously [44]. The dose of AAV vector used for the efficient transgene production *in vivo* is usually selected empirically, and may not correlate with the efficiency of the transduction *in vitro*. Due to the complex relationship between the dose of the AAV vector and the plasma concentration of the transgenic protein, data obtained *in vitro* do not often accurately predict the results *in vivo*. Not only the vector design, transduction efficiency, and the ratio of transducing cells to the vector dose affect the production of the transgenic protein. Animal physiology and even immune response may also impact on the duration of the transgenic protein expression and its lifetime in plasma [44].

The experimental animals were euthanized 7 weeks after the second vaccination. The transgene expression delivered with AAV vectors typically takes several weeks to reach its maximum level. Then it wanes due to the subsequent loss of the AAV vectors not integrating into the cellular genome. Concurrently, specific T-cell response and memory cells are formed during this time [10].

The Splenocyte Subpopulation Analysis after Vaccination

Viral vectors can initiate T-cell mediated immune response both to viral antigens including capsid proteins and to a transgene presented by MHC molecules on APCs [31]. Splenocytes isolated from the mouse spleens were analyzed with the flow cytometry to examine the lymphocyte subpopulations of the spleens. We performed immunophenotyping and determined the relative

numbers of CD4+ T-cells in the CD3+ T-cell gate, activated CD4+CD25+ T-cells in the CD4+ T-cell gate, and regulatory T-cells (Tregs) by FoxP3 and CD25 co-expression and by the absence of CD127 expression. The representative immunophenotyping data are shown in Figure 1. FSC profiles on the FSC/SSC dot plots (Figure 1A) demonstrate the appearance of the larger cells among the lymphocytes of the immunized animals, particularly in the group immunized with the AAV-mPTH-GPI vector, which possibly indicates the occurrence of the activated reactive lymphocytes.

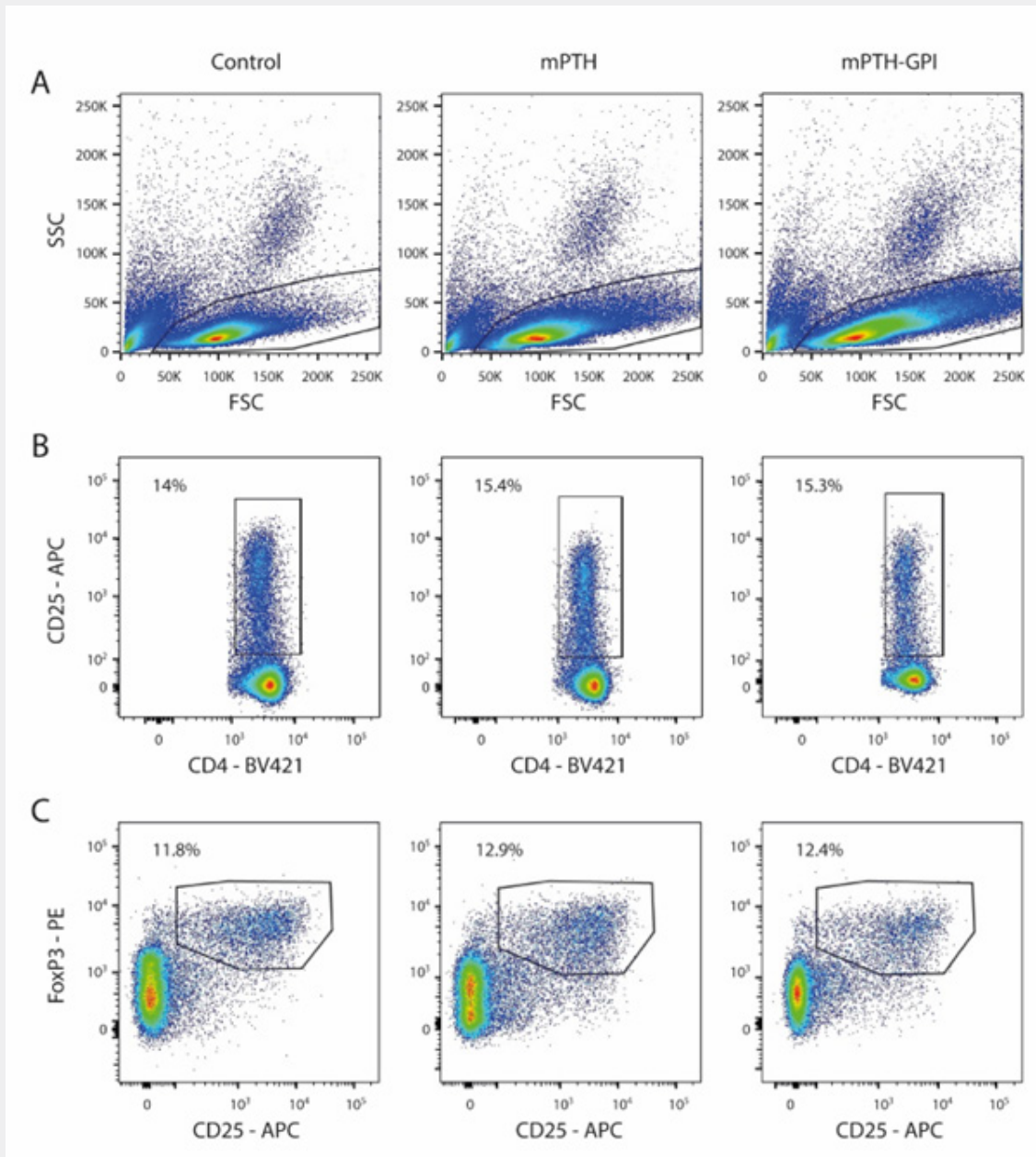


Figure 1: The phenotypic characteristics of lymphocytes isolated from the spleens of control and immunized animals. (A) FSC/SSC dot plots built from the single events to separate the lymphocyte population from the other splenocytes and debris area. (B) CD4/CD25 dot plots built from CD4+ T-cells to isolate activated CD4+CD25+ T-cells. (C) CD25/FoxP3 dot plots built from CD4+ T-cells to identify regulatory T-cells with the CD25+ FoxP3+ phenotype.

Table 1: The relative number of lymphocyte subpopulations in the mice spleens. The asterisk stands for as follows: * - p<0.05 between control and mPTH-GPI groups, ** - p<0.05 between control and mPTH groups, *** - p<0.05 between mPTH and mPTH-GPI groups.

	CD4+ T-cells, %	CD4+CD25+ activated T-cells, %	CD25+FoxP3+ regulatory T-cells, %	CD25+CD127neg regulatory T-cells, %
Control (n=5)	57.1, [55.5; 57.4] *	14, [13.5; 14.4] *	11.8, [11.3; 12.7]	12.1, [11.9; 13]
mPTH (n=5)	56, [55.2; 57.4] ***	15.4, [14.8; 16.5]	12.9, [12.1; 13.2]	13.3, [11.3; 13.5]
mPTH-GPI (n=5)	51.8, [50.9; 51.9] *&***	15.3, [14.9; 16] *	12.4, [12.3; 12.6]	13, [12.5; 13.1]

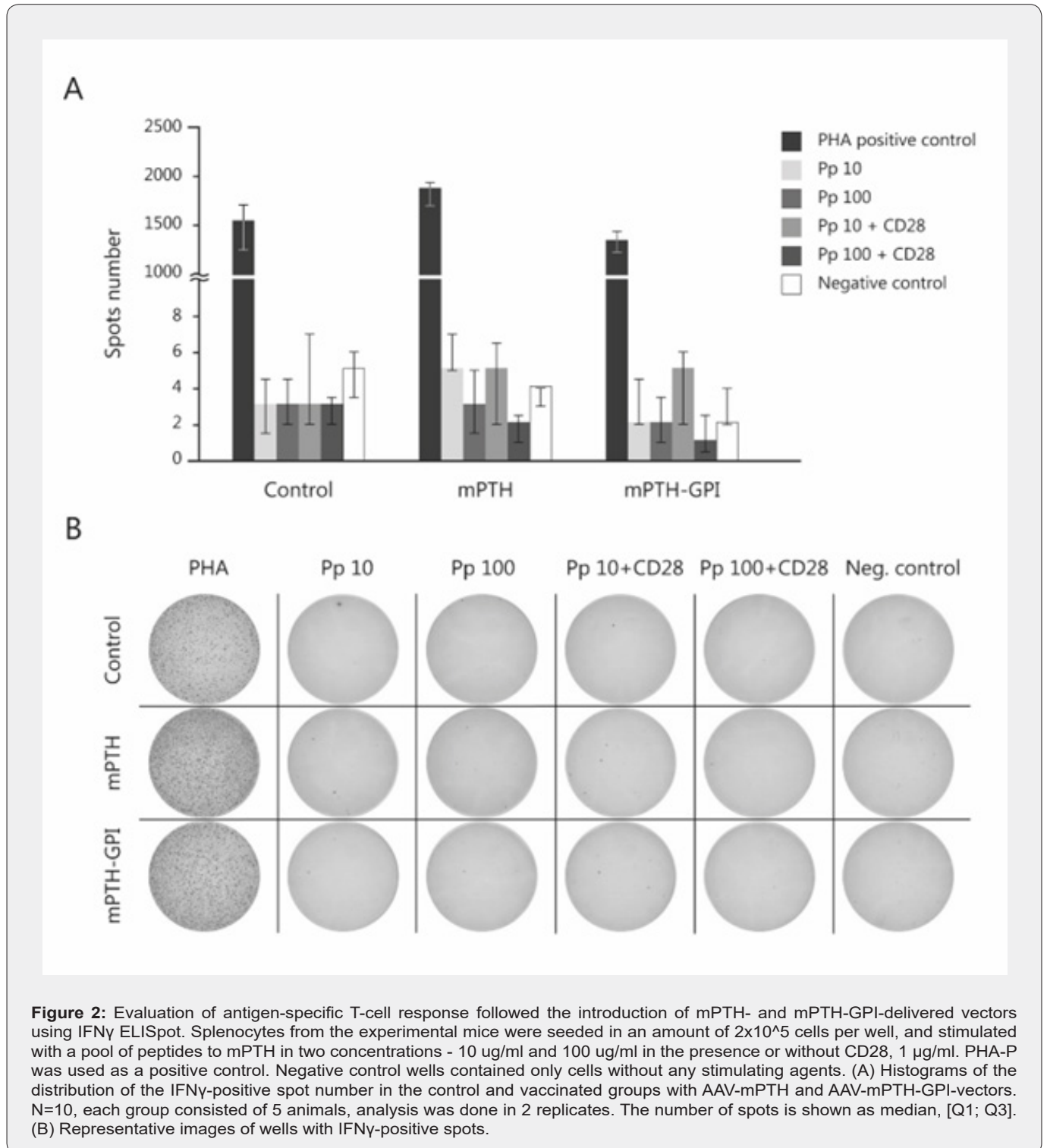


Table 2: The frequency of cells in each generation of divided cells after stimulation of splenocytes with anti-CD3/CD28 beads for 3 days. Data are presented as median, [Q1; Q3]. Significant differences of the frequency of cells between groups for each generation are indicated with an asterisk (*). * - $p < 0.05$ between control and mPTH-GPI, ** - $p < 0.05$ between control and mPTH; no significant differences were found between mPTH and mPTH-GPI.

	Generation 1, %	Generation 2, %	Generation 3, %	Generation 4, %
Control (n=10)	13.35, [13.3; 13.63] *&**	25.55, [23.03; 25.68]*	25.25, [20.08; 28.33] *	9.27, [7.71; 10.05] *&**
mPTH (n=10)	16.2, [15.9; 16.3]**	21.1, [21.1; 26.9]	22.8, [18.8; 26.1]	5.94, [2.87; 6.1]**
mPTH-GPI (n=10)	16.85, [15.8; 17.98]*	12.8, [11.83; 14.08]*	6.48, [5.81; 6.83] *	1.41, [1.24; 2.99]*

The AAV-mPTH vector vaccination didn't have a significant impact on the relative number of CD4+ T-cells compared to the control ($p = 0.9841$) (Table 1). At the same time, AAV-mPTH-GPI immunization led to a significant decrease in the relative number of CD4+ T-cells to 51.8% compared to 57.1% of the control ($p = 0.0079$). It is of note that there were significant differences in the number of CD4+ T-cells ($p=0.0079$) between both vaccinated groups. We observed a slight increase in the number of activated CD4+CD25+ T-cells reaching up to 15.4% for the splenocytes of mice vaccinated with AAV-mPTH-vector and up to 15.3% for the AAV-mPTH-GPI group of mice compared to 14% in the control group (Figure 1B), however, only the AAV-mPTH-GPI group had significant differences with the control ($p=0.0079$). The differences of the number of activated CD4+CD25+ T-cells between the control and the AAV-mPTH group ($p = 0.1032$), as well as between both vaccinated groups ($p = 0.9524$) were not significant (Figure 1B, Table 1). Also, there was no significant difference in the number of regulatory T-cells that expressed CD25+FoxP3+ and CD25+CD127low between the experimental groups, $p > 0.05$ (Figure 1C, Table 1).

Assessment of the vaccine's immunogenic potential

Two methods were used to assess the vaccine's capacity to induce a specific T-cell immune response: flow cytometry and IFN- γ ELISpot, an enzyme-linked immune spot. ELISpot is a common method for monitoring the T-cell response to a target gene in gene therapy. Using IFN- γ ELISpot we assessed IFN γ , a cytokine secreted by T-cells in response to stimulation. Prior to ELISpot splenocytes were defrosted and placed in a CO₂ incubator overnight.

As it is known that short (<15 amino acids) peptides are not subject to be processed by APC, and can be efficiently bound to MHC class I molecules on the surface of all nucleated cells, we stimulated splenocytes via adding a pool of mPTH peptides at two concentrations, 10 $\mu\text{g/ml}$ and 100 $\mu\text{g/ml}$. 10 peptides were chosen out of 26 - peptides numbered from 8 to 17 in the list of Table S1. Selecting the peptides for the experiment we considered not only their ability to bind to MHC molecules, but also their physicochemical properties, including charge and solubility. Thus, due to their amino acid content, peptides numbered 1,2,3 are hydrophobic, and would require an organic solvent for their dissolution, while peptides with numbers 7-17 can be easily dissolved in water. Peptides numbered 5-6 and 18-20 would require acidification, while peptides with numbers 22-25 would need alkalization to be fully dissolved. Therefore, we choose those peptides that might be bound to MHC molecules with the highest

affinity, and, at the same time, could be dissolved in the same solvent, water. Our peptide pool appeared to be neutral with a low basicity and, with a net charge ranged from +0.086 to +3.086. The final concentration of our 10-peptide pool was 10 $\mu\text{g/ml}$ and 100 $\mu\text{g/ml}$, while the concentration of each individual peptide was 1 $\mu\text{g/ml}$ and 10 $\mu\text{g/ml}$, respectively. Also, some wells with peptide-stimulated cells were costimulated by CD28 to enhance T-cell receptor stimulation. The representative ELISpot data are shown in Figure 2.

Flow cytometry was used to evaluate the proliferative potential of splenocytes following both specific (a pool of peptides to mPTH) and nonspecific challenges (anti-CD3/CD28 beads). We stained splenocytes with CFSE to monitor their divisions after stimulation. Figure 3A demonstrates representative CFSE histograms of cell proliferation after stimulation with anti-CD3/CD28 beads for 3 days. CFSE histogram profile of splenocytes from the mice vaccinated with the AAV-mPTH-GPI-vector is crucially different from those of control mice or the mice immunized with the AAV-mPTH vector. The percentage of the divided cells in these groups is also different. Splenocytes from the mice vaccinated with the AAV-mPTH-GPI-vector divided more slowly (Figure 3B). There were only 43% of the divided cells in this experimental group by the third day of the analysis, while the control group of mice demonstrated 79.4% of the divided cells, and 77.6% were in the group of the splenocytes from the mice vaccinated with the AAV-mPTH-vector. The differences in the cell frequencies were significant between the control and mPTH-GPI groups ($p = 0.0022$), There were no significant differences between the mPTH and control group ($p = 0.697$) and between the mPTH-GPI and mPTH groups ($p = 0.1255$).

To interpret the results, we performed the additional analysis of the CFSE histogram data using the approach proposed by Roederer [45]. Since cells divide exponentially, CFSE histogram analysis is not straightforward. For instance, one cell that has divided 4 times will produce 16 new cells in the 4th generation, but 4 cells that have divided twice will also produce 16 cells, but in the second generation [45]. Taking into account that each new degeneration of the divided cells differs from the previous one by two-time-lower CFSE intensity, we split CFSE-histograms for the proliferating cells into 4 generations to obtain the frequencies of cells in each new generation (Figure 3D), and summarized them in such a way to obtain the frequency of cells that divided at least once, twice, etc. (Figure 3C). Thus, to calculate the number of cells that divided at least once, we summed up the events of the 1st, 2nd, 3rd and 4th generations. To calculate the number of cells that

divided at least twice, we summed up the events of the 2nd, 3rd and 4th generations, etc. In total, we were able to resolve four new generations for the divided cells. Since we did not measure the absolute number of cells, we operated with the cell frequencies rather than to process the number of cells (cytometric events), to compare the data between different groups.

Comparing the frequency of cells in each generation among the three experimental groups (Figure 3D), we found that for the control group as well as for the group vaccinated with the AAV-mPTH-vector the maximal frequency of divided cells was in the second and the third generations, while the largest frequency of divided cells for the splenocytes from the AAV-mPTH-GPI group was in the first generation, i.e. among cells that divided only 1 time. Further, for this group, the frequency of cells that have

divided 2 or more times decreases. We assume that the differences in the prevalent frequency of a particular cell generation for the splenocytes from different experimental groups can arise from a fundamentally different initial composition of cell subsets in the total population of splenocytes that might be formed in response to the vaccination and proliferate at different rates. Frequency of cells in each generation of divided cells and significance of the differences are represented in Table 2. By comparing the frequency of cells that have divided at least several times (Figure 3C), we observed that the frequency of cells from mPTH-GPI group that have divided no less than any number of times was always smaller and significantly differed from that of from the control or mPTH group (Table 3).

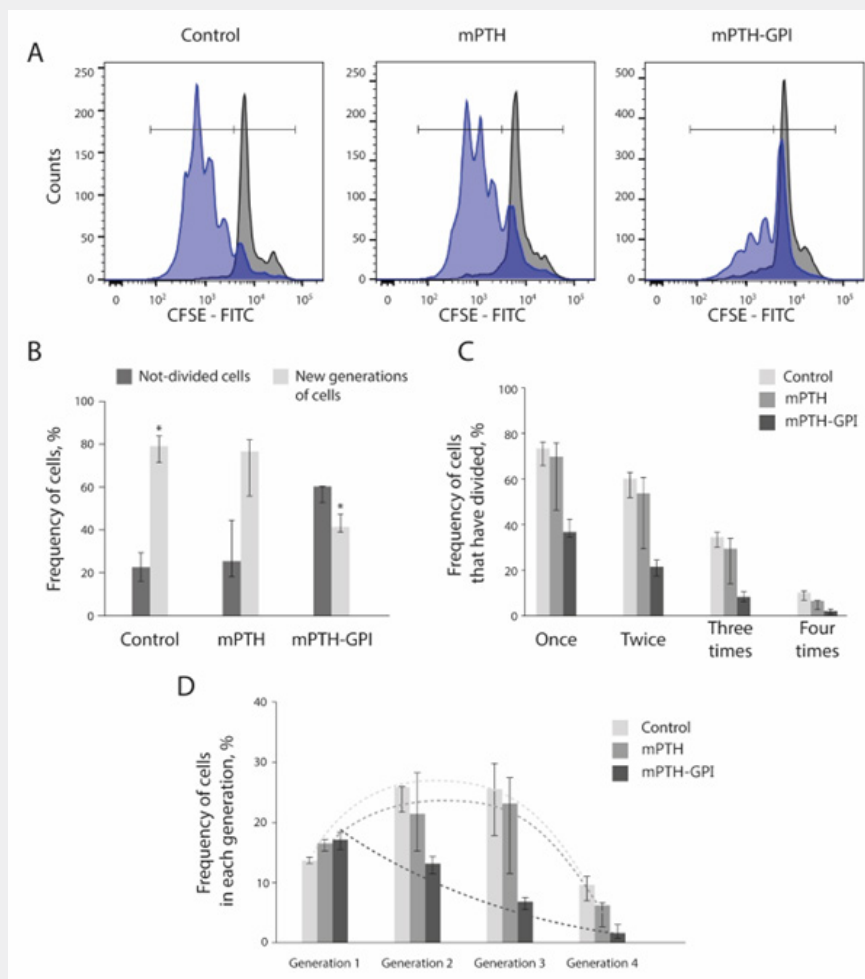


Figure 3: Splenocyte response to the nonspecific stimulation with anti-CD3/CD28 beads. (A) Representative CFSE histogram profiles of proliferated splenocytes from the control, AAV-mPTH, and AAV-mPTH-GPI groups in response to the activation with anti-CD3/CD28 beads. The blue graph stands for the splenocytes stimulated for 3 days; the gray is for the non-stimulated splenocytes maintained in culture for 3 days. The intervals show the gating regions used for separating divided and undivided cell populations. (B) Frequency histograms of the divided (light-colored) and not-divided cells (dark-colored) in response to the nonspecific stimulation in the three groups in study (n=10). Data are presented as median, [Q1; Q3]. Significant differences between groups in the number of divided cells are indicated with an asterisk (*). $p = 0.0022$ between mPTH-GPI and control, $p = 0.697$ between mPTH and control, $p = 0.1255$ between mPTH-GPI and mPTH. (C) Histogram of the cell frequency that divided at least a certain number of times. (D) Histogram of the cell frequency in each generation of divided cells among the 3 groups.

Table 3: The frequency of cells that divided at least several times after stimulation of splenocytes with anti-CD3/CD28 beads for 3 days. Data are presented as median, [Q1; Q3]. Significant differences of the frequency of cells between groups for the cells that have divided at least a certain number of times are indicated with an asterisk (*). * - $p < 0.05$ between control and mPTH-GPI, ** - $p < 0.05$ between control and mPTH; no significant differences were found between mPTH and mPTH-GPI.

	Frequency of cells that have divided at least once, %	Frequency of cells that have divided at least twice, %	Frequency of cells that have divided at least three times, %	Frequency of cells that have divided at least four times, %
Control (n=10)	72.89, [69.27; 74.3] *	59.54, [55.92; 61.02] *	33.89, [32.87; 34.57]*	9.27, [7.71; 10.05]*&**
mPTH (n=10)	69.34, [60.87; 71.7]	53.14, [42.77; 55.8]	28.9, [21.67; 32.04]	5.94, [2.87; 6.1] **
mPTH-GPI (n=10)	36.13, [34.9; 40.54] *	20.72, [18.41; 23.41] *	7.42, [6.47; 9.33] *	1.41, [1.24; 2.99] *

To assess the immunogenicity of the transgene, splenocytes from the three experimental groups were also stained with CFSE and stimulated with a pool of peptides to mPTH in two doses - 10 and 100 $\mu\text{g/ml}$. 3 days later after stimulation we analyzed CFSE histograms to monitor the proliferation of mPTH-specific lymphocytes. But we found no new generations of dividing mPTH-specific T cells and any significant differences compared with the unstimulated cells (Figure S3).

Discussion

At present, immunotherapy combined with genetic engineering methods is one of the cutting-edge approaches in cancer treatment. Depending on the cell type affected by malignant transformation and its immune microenvironment, and the dynamic evolution of crosstalk between transformed cells and microenvironment, every tumor requires different immunotherapeutic strategies. The challenge of immunotherapy is to break immune tolerance to a patient's tumor antigens so that to induce the antitumor immune response and to maintain it for a prolonged period. In some cases, tumor cells are modified using transfer of a therapeutic gene, its fragments or oligonucleotides so as for the tumor cells to be destroyed or become recognizable for the immune attack [32,46,47], while in other cases *ex vivo* manipulation of some immune cells (dendritic cells, NK-cells or cytotoxic lymphocytes) is performed to specifically direct these cells against tumor antigens [4,48].

We constructed AAV-vectors that encode murine PTH in two variants: in a native secreted form (AAV-mPTH) and in a modified GPI-anchored form (AAV-mPTH-GPI) attaching a GPI-anchor signal sequence to mPTH gene that would convert it to a protein retained on the membrane of the transduced cells that could be of any type including prevalent myocytes of muscle fibers and rare professional antigen-presenting cells (APC) in a case of intramuscular vaccine injection. We observed that vaccination with AAV-mPTH induced neither generation of PTH-specific T-cells secreting IFN γ nor proliferation of PTH-specific clones in our *in vitro* experiments with splenocytes isolated 7 weeks after the booster mouse immunization and stimulated with a mix of synthetic peptides of the murine PTH. We find it rather natural as mPTH expressed as a transgene product of an AAV-mPTH-vector is identical to the endogenous mPTH of the laboratory animals. Induction of the immune response against mPTH requires overcoming the peripheral immune tolerance to mPTH. In the

case of the mouse immunization with mPTH in a modified GPI-anchored form we didn't observe in our ELISpot experiments any rise of PTH-specific T-cells secreting IFN γ either. It means that the occurrence of mPTH located on the membranes of the transduced cells in a skeletal muscle and not presented by MHC class I appeared not sufficient to induce PTH-specific immune response that should be mediated by APC participation of the muscles.

As a matter of fact, antigen choice is a critical step during design of any antitumor vaccine. It is ideal when the antigen for a vaccine is chosen from neoantigens expressed exclusively by tumor cells and appears as a new and unique version of a mutant protein in the course of a malignant transformation [49]. PTH is not a tumor-specific neoantigen, but belongs to the class of tumor-associated antigens. Expressing endogenously, it is not immunogenic as high-affinity T-cells specific to PTH are usually eliminated at the stage of a negative selection during development of immune repertoire in the thymus. Thus, the elaboration of an effective vaccine that provokes the PTH-specific T-cell immune response requires overcoming the immune tolerance to PTH, foremost peripheral. The goal is to activate rare low-affinity PTH-specific T-cells.

On the other side, avoidance of immune activation along with a concurrent transgene expression is a known property of AAV-based vaccines that makes them principally distinct from the adenoviral vaccines [11,31]. Early publications focused on the T-cell activation in response to the AAV-vaccine antigens injected intramuscularly reported that T-cell response to the expressed transgene critically depended on the AAV-transduction efficiency of the dendritic cells (DCs) and the transgene presentation by MHC type I [12]. Intramuscular administration of recombinant AAV-vaccine induced a stable transgene (β -galactosidase) expression, and in contrast to the adenoviral vaccine that effectively transduced DCs, didn't induce activation of transgene-specific CD8+ cytotoxic T-cells as well as CD4 T helpers. Yet, however, therapy based on AAV-vectors is able to trigger both humoral and adaptive immune response to the expressed transgene [6,50], but for this goal the threshold for the efficient stimulation of DCs, their maturation and active T-cell priming should be overcome [11].

There are many factors that impact the immunogenicity of AAV-delivered transgene. The magnitude of the immune response crucially depends on the protocol of AAV administration. Route of AAV administration [9,10], promoter type, vector dose [51], capsid

serotype [6], the transgene product and its intrinsic endogenous immunogenicity [52], host species, target tissue and structure of the vector genome may exert a drastic effect on transgene-elicited immunity [11]. Also, a supraphysiological level of the transgene expression in muscles is able to break immune tolerance. Thus, the intramuscular injection of AAV-Epo-vectors that expressed a high level of erythropoietin provoked the autoimmune response to erythropoietin [53]. Vector construction, and in particular, promoter type before the transgene, can also be of great importance. If any specific promoter not active in DCs is used the estimated rate of the transgene-specific immune response would be very low. There are some strategies that may contribute to trigger the immunogenicity of AAV-delivered transgene. Thus, frequency of CpG motif content in the viral genome may regulate the immune response promoting TLR9 stimulation and initiating the innate immunity [54]. Administration of other TLRs agonists would be also favorable. Transgene incorporation into the viral capsid and incorporation of point mutation might accelerate immune response early at the stage of the viral entry into the cell or during viral recognition with cytoplasmic pattern recognition receptors (PRRs) [5]. Truncated versions of transgene are in high proportion and more readily directed to degradation during translation, and thus, might be better processed by APC leading to the more intense immune response to the transgene. Ability of AAV-vaccines to transduce APC directly is of extreme importance, that might throw away the immunotolerance barrier to self-tumor-associated antigens [6,12].

Also, repeated vaccinations along with additional stimulators of humoral and cellular immunity such as agonists of co-stimulation molecules on APCs (e.g. OX-40), immune check-point inhibitors (often CTLA-4, PD-1) increases the chances of successful and stable immune response against tumor maintained for a prolonged period [48]. Lots of efforts are focused at development of new adjuvants that would stimulate non-specific immunity via PRRs and TLRs. Booster vaccination and mPTH attached on the cell surface of the transduced cells via GPI-anchor didn't help in provoking immune response against mPTH. Therefore, we suggest that future experiments with the development of a vaccine against mPTH should consider the factors mentioned above to improve its immunogenicity to the transgene.

Cellular microenvironment of skeletal muscles may also predetermine the immune response initiated upon vector immunization [55]. Injected intramuscularly AAV-vectors travel along the tissue of skeletal muscle containing multiple cell types, with myocytes forming muscle fibers, endothelial cells and fibroblasts prevailing. Myosatellite cells, myoblasts, DCs and macrophages are present in a far lesser number [56]. If a vector transduces APC, the vector transgene might be presented by MHC type I on the APC surface, inducing activation of the transgene-specific T-cells. Yet, numerous studies demonstrate the poor efficiency of APC transduction by AAV-vectors, and by AAV2 serotype, in particular [29,30]. In addition to it, the survival time of transduced APCs is too short for the AAV-vectors to

propagate, yet AAV-vectors do not replicate in APC and cannot not propagate to transduce other cells. Little is known on the immune response if other cells than APCs are transduced. It has been shown that CD8+ T-cells priming does not necessarily depend on antigen processing in AAV-transduced DCs [57]. CD8 T-cell response against a transgene that continuously expressed in muscle myocytes can be primed due to the cross-presentation by APCs that acquire the transgene from the muscles and present it to CD8 T-cells by MHC class I [58,59]. It is known that the cross-presentation of exogenous antigens that are cross-presented by MHC class I often results in CD8+ T-cell tolerance [57].

There are numerous publications on the induced immune tolerance to the transgene in response to the immunization with AAV-vectors [27-30,60] which may occur due to the suppression, anergy, apoptotic death or functional exhaustion of CD8+ T-cells. It's worth noting that muscle tissue is characterized by weak transduction efficiency of muscle APCs, the lack of MHC class I expression increase on transduced cells other than APCs and T-cells exhaustion [30]. It's of great interest that in response to the non-specific challenge we observed the delayed proliferation kinetics of T-splenocytes isolated from the mice immunized with AAV-mPTH-GPI-vectors that held mPTH attached to the membranes of the transduced cells. We suggest that constant mPTH availability on the cell surface, mostly of myocytes because of their prevalence in muscle tissue, might initiate the weak activation of PTH-specific T-lymphocytes via cross-presentation by DCs [58,59]. In the absence of co-stimulated signals or proinflammatory microenvironment such weak T-cell activation might induce either T-cell anergy, or increase their activation threshold that makes them either inactive or activating with a lower rate in case of a stable but not strong enough tonic DCs activation, which leads, in the long run, to their tolerant phenotype [61,62].

Most certainly, the ratio of different lymphocyte subpopulations among splenocytes as well as availability of T-cell clones and TCR-repertoire might differ between experimental groups and particularly in AAV-mPTH-GPI splenocytes. As different lymphocyte subpopulations respond with different kinetics to the stimulation, it might explain the observed effect of different proliferation kinetics in the experimental groups [63]. In our experiments we observed that it was not PTH-specific but polyclonal T-cell stimulation with CD3/CD28 beads revealed a lower activation rate of T-cells. Tregs expressing TGF β , IL-10 and other suppressive molecules could participate in the tolerance development [64], but we didn't detect significant differences in the number of regulatory CD4+CD25+CD127neg and CD4+CD25+FoxP3+ Tregs in our experiments (Figure 1C). Yet, the role of Tregs in tolerance induction cannot be ruled out as they are effective in low numbers whereas antigen-specific cells usually present in a very low number [64]. Moreover, we observed a trend of Tregs increase. It's interesting that immunization with AAV-mPTH-GPI (and with AAV-mPTH also) is followed by a significant rise of CD4+CD25+ T-cells number (Figure 1B, Table 1). FSC/SSC

dot plots showing the distribution of cells based upon size showed the larger size of lymphocytes isolated from mice immunized with AAV-mPTH-GPI-vector (Figure 1A), which implicitly suggests the cells activation. Thus, activation splenocyte threshold seems also conceivable, as splenocytes after mice immunization might be set in the context of the stable and long-lasting transgene expression as during chronic persistent infection. The functional exhaustion of T-cells cannot be ruled out either.

Therefore, our work is the first step in the elaboration of the gene-therapy vaccine against PC based on a dual immunization with AAV-vectors (AAV2/2 and AAV2/9 serotypes) against PTH expressed either in a native secreted form or in a GPI-anchored form. We studied the vectors' immunogenicity in response to the library of PTH synthetic peptides, the affinity of which with MHC molecules was assessed by us *in silico*. We revealed that the vector constructs used by us were not immunogenic, but induced the polyclonal immune tolerance to T-cells. Induction of tolerance to the transgene expressed endogenously in response to the

immunization with AAV-vectors was expectable and highlighted in many publications [27-31]. The elaboration of onco-vaccines against tumor-associated antigens and, in particular, the elaboration of the gene-therapy vaccine against PC require overcoming the immune tolerance, which is possible by varying a range of factors such as genetic modification of the vector construct and the immunization with various serotypes [6,60], usage of strong adjuvants that could stimulate the non-specific part of the immunity (PPRs, TLRs), or the addition of agonists against co-stimulatory molecules on APCs (e.g. OX-40, CD40L), or the application of immune check-point inhibitors (mostly used CTLA-4, PD-1) [48]. For the goal of strengthening the immune response we used the GPI-anchored form of PTH and a booster vaccination, but both approaches gave rise to polyclonal immune tolerance. We think it would be very important in future to assess the other factors mentioned above on the immunogenicity of the genetic constructs of AAV-mPTH and AAV-mPTH-GPI-vectors.

Supplement

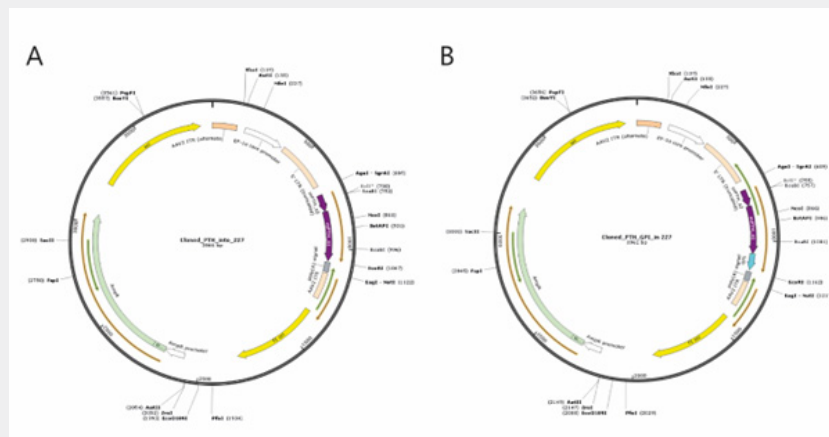


Figure S1: Plasmids expressing murine PTH (mPTH) both in the absence (A) and presence (B) of a GPI anchor signaling sequence (A and B respectively).

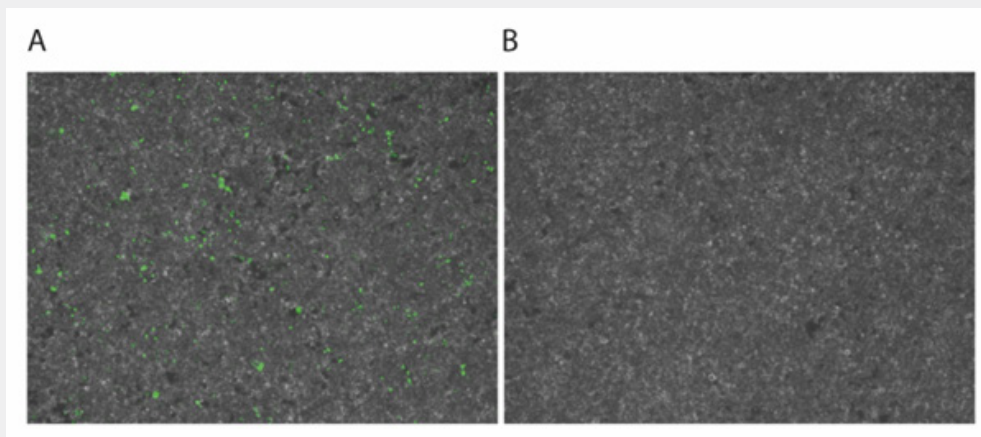


Figure S2: HEK293T cells transduced with AAV-vectors at a dose of 20,000 viral genomes per cell (vg). A. Transduction with AAV-mPTH-GFP; B. Transduction with AAV-mPTH.

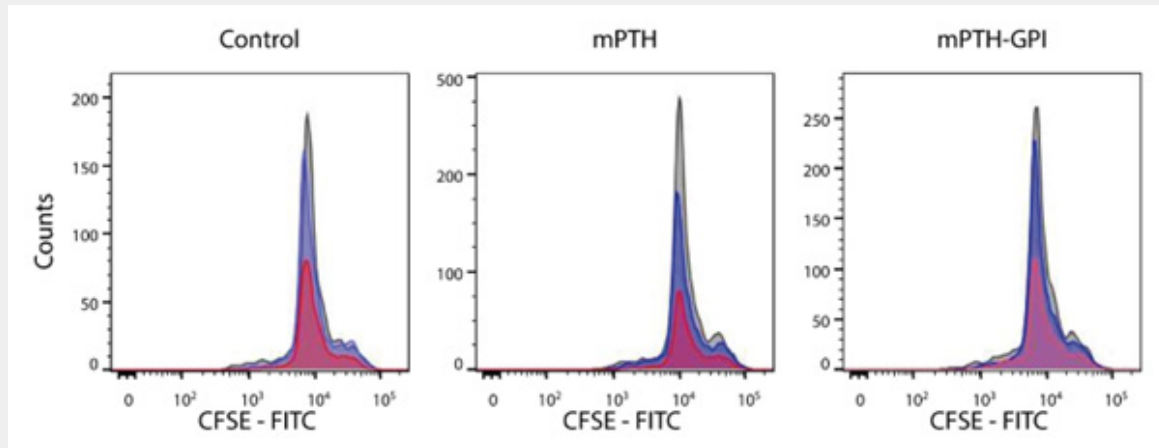


Figure S3: Representative CFSE histograms of the splenocyte proliferative response (control mice, vaccinated with AAV-mPTH-GPI or AAV-mPTH) to specific challenge with a pool of mPTH peptides; gray - unstimulated splenocytes; blue – splenocytes activated with the pool of peptides in the total concentration of 10 mg; red - splenocytes activated with the pool of peptides in the total concentration of 100 mg.

Figure S1: Plasmids expressing murine PTH (mPTH) both in the absence (A) and presence (B) of a GPI anchor signaling sequence (A and B respectively); Figure S2: HEK293T cells transduced with AAV-vectors at a dose of 20,000 viral genomes per cell (vg). A. Transduction with AAV-mPTH-GFP; B. Transduction with AAV-mPTH; Figure S3: Representative CFSE histograms of the splenocyte proliferative response (control mice, vaccinated with AAV-mPTH-GPI or AAV-mPTH) to specific challenge with a pool of mPTH peptides; gray – unstimulated splenocytes; blue – splenocytes activated with the pool of peptides in the total concentration of 10 mg; red - splenocytes activated with the pool of peptides in the total concentration of 100 mg; Table S1: Amino acid sequence of the peptides to mPTH. Peptides 8-17.

Funding

This research was funded by the Ministry of Science and Higher Education of the Russian Federation (agreement No. 075-15-2022-310 from 20 April 2022).

References

- Smith BK, Collins SW, Conlon TJ, Mah CS, Lawson LA, et al. (2013) Phase I/II Trial of adeno-associated virus-mediated alpha-glucosidase gene therapy to the diaphragm for chronic respiratory failure in Pompe Disease: Initial safety and ventilatory outcomes. *Human Gene Ther* 24(6): 630-640.
- Samelson-Jones BJ, George LA (2023) Adeno-associated virus gene therapy for hemophilia. *Ann Rev Med* 74: 231-247.
- Ong T, Pennesi ME, Birch DG, Lam BL, Tsang SH (2019) Adeno-associated viral gene therapy for inherited retinal disease. *Pharma Res* 36(2): 34.
- Akbulut H (2020) Immune gene therapy of cancer. *Turkish J Med Sci* 50: 1679-1690.
- Hacker UT (2023) On the way to developing AAV-based vaccines as novel tools for cancer immunotherapy. *Mol Ther Methods Clin Dev* 28: 394-395.
- Krotova K, Kuoch H, Caine C, Aslanidi G (2023) Tumor antigen-loaded AAV vaccine drives protective immunity in a melanoma animal model. *Mol Ther Methods & Clin Dev* 28: 301-311.
- Manno CS, Pierce GF, Arruda VR, Glader B, Ragni M, et al. (2006) Successful transduction of liver in hemophilia by AAV-Factor IX and limitations imposed by the host immune response. *Nature Med* 12(3): 342-347.
- Calcedo R, Kuri-Cervantes L, Peng H, Qin Q, Boyd S, et al. (2017) Immune responses in 101HEMB01, a Phase 1/2 open-label, single ascending dose-finding trial of DTX101 (AAVrh10FIX) in patients with severe hemophilia B. *Blood* 130(Suppl 1): 3333.
- Brockstedt DG, Podsakoff GM, Fong L, Kurtzman G, Mueller-RW, et al. (1999) Induction of immunity to antigens expressed by recombinant adeno-associated virus depends on the route of administration. *Clin Immunol* 92(1): 67-75.
- Cao O, Hoffman BE, Moghimi B, Nayak S, Cooper M, et al. (2009) Impact of the underlying mutation and the route of vector administration on immune responses to factor IX in gene therapy for hemophilia B. *Mol Ther* 17: 1733-1742.
- Mays LE, Wilson JM (2010) The complex and evolving story of T cell activation to AAV vector-encoded transgene products. *Mol Ther* 19(1): 16-27.
- Jooss K, Yang Y, Fisher KJ, Wilson JM (1998) Transduction of dendritic cells by DNA viral vectors directs the immune response to transgene products in muscle fibers. *J Virol* 72: 4212-4223.
- Rodrigo JP, Hernandez-PJC, Randolph GW, Zafereo ME, Hartl DM, et al. (2020) Parathyroid cancer: An update. *Cancer Treatment Rev* 86: 102012.
- Bilezikian JP, Cusano NE, Khan AA, Liu JM, Marcocci C, et al. (2016) Primary hyperparathyroidism. *Nature Rev Dis Prim* 2: 1-16.
- Marini F, Giusti F, Palmini G, Aurilia C, Donati S, et al. (2023) Parathyroid carcinoma: update on pathogenesis and therapy. *Endocrines* 4: 205-235.
- Dedov II, Melnichenko GA, Mokrysheva NG, Rozhinskaya LY, Kusnezov NS, et al. (2016) Primary hyperparathyroidism: the clinical picture, diagnostics, differential diagnostics, and methods of treatment. *Problem Endocrinol* 62(6): 40-77.

17. Teleanu MV, Fuss CT, Paramasivam N, Pirmann S, Mock A, et al. (2023) Targeted therapy of advanced parathyroid carcinoma guided by genomic and transcriptomic profiling. *Mol Oncol* 17(7): 1343-1355.
18. Bradwell AR, Harvey TC (1999) Control of hypercalcaemia of parathyroid carcinoma by immunisation. *Lancet* 353(9150): 370-373.
19. Horie I, Ando T, Inokuchi N, Mihara Y, Miura S, et al. (2010) First Japanese patient treated with parathyroid hormone peptide immunization for refractory hypercalcemia caused by metastatic parathyroid carcinoma. *Endocrine J* 57(4): 287-292.
20. Betea D, Bradwell AR, Harvey TC, Mead GP, Schmidt-Gayk H, et al. (2004) Hormonal and biochemical normalization and tumor shrinkage induced by anti-parathyroid hormone immunotherapy in a patient with metastatic parathyroid carcinoma. *J Clin Endocrinol Metabol* 89(7): 3413-3420.
21. Sarquis M, Marx SJ, Beckers A, Bradwell AR, Simonds WF, et al. (2020) Long-term remission of disseminated parathyroid cancer following immunotherapy. *Endocrine* 67(1): 204-208.
22. Aichele P, Brduscha-Riem K, Zinkernagel RM, Hengartner H, Pircher H (1995) T cell priming versus T cell tolerance induced by synthetic peptides. *J Exp Med* 182: 261-266.
23. Schott M, Seissler J, Feldkamp J, von Schilling C, Scherbaum WA (1999) Dendritic cell immunotherapy induces anti-tumor response in parathyroid carcinoma and neuroendocrine pancreas carcinoma. *Hormone Metabolic Res* 31(12): 662-664.
24. Burr AM, Zuckerman PC, Castillo AB, Partridge NC, Parekkadan B (2022) Bioactive, full-length parathyroid hormone delivered using an adeno-associated viral vector. *Exp Biol Med* 247(21): 1885-1897.
25. Zhou Y, Lü BJ, Xu P, Song CF (2005) Optimising gene therapy of hypoparathyroidism with hematopoietic stem cells. *Chinese Med J* 118(3): 204-209.
26. Liu D, Zhu Y, Yang C, Long J, Yao C, et al. (2011) Potential treatment of hypoparathyroidism with recombinant plasmids encoding preproparathyroid hormone. *J Endocrinol Investigat* 35(5): 479-484.S
27. Bharadwaj AS, Kelly M, Kim D, Chao H (2010) Induction of immune tolerance to FIX by intramuscular AAV gene transfer is independent of the activation status of dendritic cells. *Blood J Am Society of Hematol* 115(3): 500-509.
28. Mingozzi F, Liu YL, Dobrzynski E, Kaufhold A, Liu JH, et al. (2003) Induction of immune tolerance to coagulation factor IX antigen by *in vivo* hepatic gene transfer. *J Clin Investigat* 111(9): 1347-1356.
29. Dobrzynski E, Mingozzi F, Liu YL, Bendo E, Cao O, et al. (2004) Induction of antigen-specific CD4+ T-cell anergy and deletion by *in vivo* viral gene transfer. *Blood* 104(4): 969-977.
30. Mays LE, Wang L, Lin J, Bell P, Crawford A, et al. (2014) AAV8 induces tolerance in murine muscle as a result of poor APC transduction, T cell exhaustion, and minimal MHCI upregulation on target cells. *Mol Ther* 22(1): 28-41.
31. Ertl HC (2021) T cell-mediated immune responses to AAV and AAV vectors. *Frontiers in Immunol* 12: 666666.
32. Selvaraj P, Yerra A, Tien L, Shashidharamurthy R (2008) Custom designing therapeutic cancer vaccines: delivery of immunostimulatory molecule adjuvants by protein transfer. *Human Vaccines* 4: 384-388.
33. Chahal PS, Schulze E, Tran R, Montes J, Kamen AA (2014) Production of adeno-associated virus (AAV) serotypes by transient transfection of HEK293 cell suspension cultures for gene delivery. *J Virol Methods* 196: 163-173.
34. Dismuke JD, Tenenbaum L, Jude Samulski R (2013) Biosafety of recombinant adeno-associated virus vectors. *Curr Gene Ther* 13(6): 434-452.
35. Sumit G, Brown AM, Jenkins C, Campbell K (2020) Viral vector systems for gene therapy: a comprehensive literature review of progress and biosafety challenges. *Applied Biosafety* 25(1): 7-18.
36. Michels A, Frank AM, Günther DM, Mataei M, Börner K, et al. (2021) Lentiviral and adeno-associated vectors efficiently transduce mouse T lymphocytes when targeted to murine CD8. *Mol Ther Methods & Clin Dev* 23: 334-347.
37. Tario JD, Muirhead KA, Pan D, Munson ME, Wallace PK (2011) Tracking immune cell proliferation and cytotoxic potential using flow cytometry. *Flow Cytometry Protocol* 699: 119-164.
38. Wang D, Tai PW, Gao G (2019) Adeno-associated virus vector as a platform for gene therapy delivery. *Nature Rev Drug Discov* 18: 358-378.
39. Heider S, Dangerfield JA, Metzner C (2016) Biomedical applications of glycosylphosphatidylinositol-anchored proteins. *J Lipid Res* 57(10): 1778-1788.
40. Muenchmeier N, Boecker S, Bankel L, Hinz L, Rieth N, et al. (2013) novel CXCL10-based GPI-anchored fusion protein as adjuvant in NK-based tumor therapy. *PLoS One* 8(8): e72749.
41. Liu L, Wen M, Zhu Q, Kimata JT, Zhou P (2016) Glycosyl phosphatidylinositol-anchored C₃₄ peptide derived from human immunodeficiency virus type 1 Gp41 is a potent entry inhibitor. *J Neuroimmune Pharmacol* 11(3): 601-610.
42. Leiker AJ, Yen TW, Eastwood DC, Doffek K, Szabo A, et al. (2012) Factors That Influence Parathyroid Hormone Half-life: Are New Intraoperative Criteria Needed? *J Surg Res* 2: 195.
43. Sikjaer T, Amstrup AK, Rolighed L, Kjaer SG, Mosekilde L, et al. (2013) PTH (1-84) replacement therapy in hypoparathyroidism: a randomized controlled trial on pharmacokinetic and dynamic effects after 6 months of treatment. *J Bone Mineral Res* 28(10): 2232-2243.
44. Burr A, Erickson P, Bento R, Shama K, Roth C, Parekkadan B (2022) Allometric-like scaling of AAV gene therapy for systemic protein delivery. *Mol Ther Methods & Clin Dev* 27: 368-379.
45. Roederer M (2011) Interpretation of cellular proliferation data: avoid the panglossian. *Cytometry Part A* 79(2): 95-101.
46. Descamps V, Duffour MT, Mathieu MC, Fernandez N, Cordier L, et al. (1996) Strategies for cancer gene therapy using adenoviral vectors. *J Mol Med* 74(4): 183-189.
47. Takahashi S, Rousseau RF, Yotnda P, Mei Z, Dotti G, et al. (2001) Autologous antileukemic immune response induced by chronic lymphocytic leukemia B cells expressing the CD40 ligand and interleukin 2 transgenes. *Human Gene Ther* 12(6): 659-670.
48. Hollingsworth RE, Jansen K (2019) Turning the corner on therapeutic cancer vaccines. *NPJ Vaccines* 4: 7.
49. Xie N, Shen G, Gao W, Huang Z, Huang C, Fu L (2023) Neoantigens: promising targets for cancer therapy. *Signal Transduction Targeted Ther* 8(1): 9.
50. Manning WC, Paliard X, Zhou S, Pat Bland M, Lee AY, et al. (1997) Genetic immunization with adeno-associated virus vectors expressing herpes simplex virus type 2 glycoproteins B and D. *J Virol* 71(10): 7960-7962.
51. Kumar SR, Hoffman BE, Terhorst C, de Jong YP, Herzog RW (2017) The balance between CD8+ T cell-mediated clearance of AAV-encoded antigen in the liver and tolerance is dependent on the vector dose. *Mol Ther* 25(4): 880-891.

52. Sarukhan A, Camugli S, Gjata B, von Boehmer H, Danos O, Jooss K (2001) Successful interference with cellular immune responses to immunogenic proteins encoded by recombinant viral vectors. *J virol* 75(1): 269-277.
53. Gao G, Lebherz C, Weiner DJ, Grant R, Calcedo R, et al. (2004) Erythropoietin gene therapy leads to autoimmune anemia in macaques. *Blood* 103(9): 3300-3302.
54. Faust SM, Bell P, Cutler BJ, Ashley SN, Zhu Y, et al. (2013) CpG-depleted adeno-associated virus vectors evade immune detection. *J Clin Investigat* 123(7): 2994-3001.
55. Boisgerault F, Mingozzi F (2015) The skeletal muscle environment and its role in immunity and tolerance to AAV vector-mediated gene transfer. *Curr Gene Ther* 15(4): 381-394.
56. Pimorady-Esfahani A, Grounds MD, McMenamin PG (1997) Macrophages and dendritic cells in normal and regenerating murine skeletal muscle. *Muscle & Nerve: Official J Am Associat Electrodiagnostic Med* 20(2): 158-166.
57. Joffre OP, Segura E, Savina A, Amigorena S (2012) Cross-presentation by dendritic cells. *Nature Rev Immunol* 12: 557-569.
58. Fu TM, Ulmer JB, Caulfield MJ, Deck RR, Friedman A, et al. (1997) Priming of cytotoxic T lymphocytes by DNA vaccines: requirement for professional antigen presenting cells and evidence for antigen transfer from myocytes. *Mol Med* 3(6): 362-371.
59. Xu D, Walker CM (2011) Continuous CD8+ T-cell priming by dendritic cell cross-presentation of persistent antigen following adeno-associated virus-mediated gene delivery. *J Virol* 85(22): 12083-12086.
60. Mays LE, Vandenberghe LH, Xiao R, Bell P, Nam HJ, et al. (2009) Adeno-associated virus capsid structure drives CD4-dependent CD8+ T cell response to vector encoded proteins. *J Immunol* 182(10): 6051-6060.
61. Grossman Z, Paul WE (2001) Autoreactivity, dynamic tuning and selectivity. *Curr Opin Immunol* 13(6): 687-698.
62. Bijker MS, van den Eeden SJ, Franken KL, Melief CJ, van der Burg SH, et al. (2008) Superior induction of anti-tumor CTL immunity by extended peptide vaccines involves prolonged, DC-focused antigen presentation. *Eur J Immunol* 38(4): 1033-1042.
63. Iezzi G, Karjalainen K, Lanzavecchia A (1998) The duration of antigenic stimulation determines the fate of naive and effector T cells. *Immunity* 8(1): 89-95.
64. Cao O, Dobrzynski E, Wang L, Nayak S, Mingle B, et al. (2007) Induction and role of regulatory CD4+ CD25+ T cells in tolerance to the transgene product following hepatic *in vivo* gene transfer. *Blood. J Am Society Hematol* 110(4): 1132-1140.

Supplementary Materials

Table S1: Amino acid sequence of the peptides to mPTH. Peptides 8-17, highlighted in bold were used in the experiment.

Number	Peptide sequence
1	MMSANTVAKVMIIML
2	NTVAKVMIIMLAVCL
3	KVMIIMLAVCLLTQT
4	IMLAVCLLTQTDGKP
5	VCLLTQTDGKPVRRR
6	TQTDGKPVRRKRAVSE
7	GKPVRRKRAVSEIQLM
8	RKRAVSEIQLMHNLG
9	VSEIQLMHNLGKHLA
10	QLMHNLGKHLASMER
11	NLGKHLASMERMQWL
12	HLASMERMQWLRRLK
13	MERMQWLRRLQDMH
14	QWLRRLQDMHNFVS
15	RKLQDMHNFVSLGVQ
16	DMHNFVSLGVQMAAR
17	FVSLGVQMAARDGSH
18	GVQMAARDGSHQKPT
19	AARDGSHQKPTKKEE
20	GSHQKPTKKEENVLV
21	KPTKKEENVLVDGNP
22	KEENVLVDGNPKSLG
23	VLVDGNPKSLGEGDK

24	GNPKSLGEGDKADVD
25	SLGEGDKADVDVLVK
26	GDKADVDVLVKSKSQ



This work is licensed under Creative Commons Attribution 4.0 License
DOI: [10.19080/CTBEB.2024.23.5560101](https://doi.org/10.19080/CTBEB.2024.23.5560101)

**Your next submission with Juniper Publishers
will reach you the below assets**

- Quality Editorial service
- Swift Peer Review
- Reprints availability
- E-prints Service
- Manuscript Podcast for convenient understanding
- Global attainment for your research
- Manuscript accessibility in different formats
(Pdf, E-pub, Full Text, Audio)
- Unceasing customer service

Track the below URL for one-step submission
<https://juniperpublishers.com/online-submission.php>